RESEARCH ARTICLE OPEN ACCESS

Highly porous web network of Mn doped ZnO for ammonia gas sensor

K S Pakhare[1,2], B M Sargar [1,*], S. S. Potdar[3,4], A.K. Sharma[3]
[1,] DIST-FIST Sponsored material research laboratory, Department of Chemistry, Jaysingpur College, Jaysingpur, Tal- Shirol, Dist- Kolhapur, (M.S.), India- 416101*
[2]Anandibai Raorane Arts, Commerce and Science College, Vaibhavwadi, Dist- Sindhudurg, (M.S), India – 416810
[3,4] Earth and Space Science Laboratory, Department of Physics, Shivaji University, Kolhapur- 416004, India
[4]Department of Physics, Shree Datta Polytechnic College, Shirol, Tal- Shirol, Dist- Kolhapur 415120 , India
Corresponding Author: B M Sargar

ABSTRACT
In the present work, the performance of ammonia gas sensor is reported. Un-doped and Mn doped ZnO nanoparticles were synthesized by Simple Chemical Combustion method. ZnO thin films were characterized by instrumental techniques. The X-Ray diffraction study showed formation of hexagonal wurtzite crystal structure of Un-doped ZnO while Mn doped ZnO was polycrystalline. Scanning electron microscopy revealed porous interconnected web like morphology. The pore size was increased in dopant concentration. Elemental composition was confirmed by EDAX. Optical behavior shows decrease in band gap with respect to increase in Mn concentration in ZnO. 9% Mn doped ZnO thin film showed the maximum gas response of 51.11% upon exposure to 24 ppm ammonia gas concentration at 573K temperature.
Keywords: Chemical combustion method, XRD, SEM, EDAX, Optical study, gas sensor.

Date of Submission: 15-09-2017 Date of acceptance: 28-09-2017

I. INTRODUCTION

In the recent years a great deal of research efforts were directed towards the development of miniaturized gas-sensing devices, mostly for toxic gas detection and for pollution monitoring. With the increasing demand for better gas sensors in respect with sensitivity and greater selectivity, concentrated efforts are being made to find more suitable materials with the required surface and bulk properties for use in gas sensors. More significant work on the semiconducting materials as gas sensor has been extensively documented by many researchers in past few years. Semiconducting Metal oxides like SnO_2, WO_3, In_2O_3, ZnO, Cu_2O, TiO_2, CeO_2 were used for the detection of the gases [1-6]. Unfortunately, the high temperature required for the surface reactions to take place also these materials show less stability at this higher temperature. Gas-sensing performance can be enhanced by doping of impurity such as iron [7] and Tin [8-9], which not only promotes gas sensitivity but also improves the response time. Addition of dopant largely affects on morphology as well as their properties [10-13].

In our earlier research paper we have already reported the synthesis, characterization and and gas response for LPG [14]. In present work, Mn-doped ZnO nanoparticles were synthesized by chemical combustion method and compared it with synthesized pure ZnO. This method is simple, rapid, time consuming, cost effective, easy to handle and gives better results. The effect of Mn sensitization was systematically investigated at different operating temperature and gas concentration. It has been observed that addition of dopant results enhanced ammonia gas response. The synthesized films have been characterized by various techniques like XRD, SEM, EDAX, UV-Visible spectroscopy, etc. to check their properties and finally applied for the ammonia gas response study.

II. MATERIALS AND METHODS

2.1 Materials

Zinc Nitrate [$Zn(NO_3)_2.5H_2O$], Manganese Nitrate [$Mn(NO_3)_2$], and Glycin were purchased from Thomas Baker chemicals and used without further purification.

2.2 Procedure

Un-doped and Mn doped ZnO were synthesized by a chemical combustion method. 100 ml of 0.3 N solution of Glycine and Nitrates of Zn and Mn were prepared separately in a 100 ml volumetric flask. Then these prepared solutions were mixed together in exact proportion in crystalline dish

(as shown in table 1) and then it was stirred well for an hour. Then this mixed bath of solutions was allowed to keep over a hot plate for auto combustion at temperature 473 K. After the complete evaporation of water, a reddish black colored thick gel was formed, it was subsequently ignited to give a final dark brown colored Mn doped ZnO oxide product. Then, synthesized samples were annealed at temperature 673K for 2 hours and then samples were coded as Z0, MZ1, MZ2, MZ3 for un-doped ZnO, 3, 6, 9 % Mn doped ZnO respectively and they were characterized by various spectroscopic techniques.In the present study, the sensorresponse of the films was determined using equation (1) [15] as ammonia possesses the properties of reducing gas. Where *R*a is the resistance of the film in air and *R*g is that upon exposure to ammonia.

$$S = (Ra - Rg)/Ra\_ \times 100\% \quad \ldots\ldots..(1)$$

Sr. No.	Code of Samples	Stoichiometry		
		$Zn(NO_3)_2$	$Mn(NO_3)_2$	Glycine
1	MZ0	100%	00%	100%
2	MZ1	97%	3%	100%
3	MZ2	94%	6%	100%
4	MZ3	91%	9%	100%

Table 1: Stoichiometry of Un-doped and Mn doped ZnO samples

2.3 Nanoparticles formation mechanism

Nanoparticles growth involves two steps. In first step dissociation of nitrate salt of Zinc and Manganese were carried out in distilled water. Solutions of appropriate concentrations had been prepared and dissolved in distilled water with continuous stirring. After 5 min, stirred solutions were converted in to water soluble hydroxides of Zinc and manganese. This reaction can be represented by following reaction mechanism "equation 2" and "equation 3".

Step I

$$Zn(NO_3)_2 + H_2O \longleftrightarrow [Zn^{2+} + 2(O^{2-} + H^+)]_{solid} + [2H^+ + 2NO_3^-] \longleftrightarrow [Zn(OH)_2] \quad \ldots.(2)$$

$$Mn(NO_3)_2 + H_2O \longleftrightarrow [Mn^{2+} + 2(O^{2-} + H^+)]_{solid} + [2H^+ + 2NO_3^-] \longleftrightarrow [Co(OH)_2] \quad \ldots.(3)$$

Step II

$$Zn(OH)_2 + Mn(OH)_2 + Glycin \xrightarrow{473K} [Zn^{2+} + 2(O^{2-} + H^+)] + [Mn^{2+} + 2(O^{2-} + H^+)] \xrightarrow{473K}$$

$$[(Zn + Mn)^{2+} + 2O^{2-}] + 2[O^{2-} + 2H^+] \xrightarrow{473K} [Zn_{(1-x)}Mn_{(x)}O] + 2H_2O + [O] \quad \ldots\ldots (4)$$

In second step glycine solution is mixed in above hydroxide solutions of Zinc and Manganese mixed solution in appropriate proportion as mentioned in table No. 1. In this reaction (4) Glycine acts as fuel. The whole solution heated over a hot plate at temperature 473K. After 2 hours, wine red coloured sol had been formed. Water vapours had released during complete combustion of reaction mixture. With continuous heating sol had ignited which resulted into dark brown coloured Manganese doped Zinc oxide nanoparticles. Nanoparticles so obtained were annelid to remove hydrated water containt.

III. RESULTS AND DISCUSSION

3.1 Structural analysis

The powder X Ray Diffraction patterns of different $Zn_{1-x}Mn_xO$ (0 _ x _ 0.9) samples are shown in Fig. 1. Synthesized samples of un-doped and Mn doped ZnO was performed on a Philips automated X-Ray diffractometer (PW-3710) equipped with crystal monochromator employing Cu-Kα radiation of wavelength 1.5406 A° in 2Θ range 20° - 80°. The XRD patterns show that the Un-doped ZnO crystal structure is hexagonal wurtzite. No reflections due to any secondary phase are detected in the XRD pattern. The peaks are observed at 2Θ values of 31.81°, 34.54°, 36.29°, 47.53°, 56.58°, 62.85° and 67.92° are corresponding to (100), (002), (101), (102), (110), (103), (112). The obtained XRD spectra matched with the [JCPDS file No.36-1451]. This confirms hexagonal wurtzite crystal structure of ZnO. The XRD results also indicates that the Mn2+ ions systematically substituted for the Zn2+ ions in the sample without altering the wurtzite structure, as shown in the Fig.1. The slight shift in the most intense peak [101] was observed with decreases in intensity as compared with un-dopedZnO. The width of the reflections increases with increasing Mn content, indicating decreasing particle size. The shifting and broadening of XRD lines with doping strongly suggest that Mn^{2+} successfully substituted into the ZnO host structure at the Zn^{2+} site. The average particle sizes were calculated from X-ray line broadening using the Scherrer "equation 5". The average values of crystalline size of the samples were calculated based on the 101 crystal plane [16]. Where, K is constant called as the shape factor = 0.94, λ is the

Wavelength, It is also constant, known as shape factor, β is Full width at half maximum (FWHM) given in radian, Θ = It is the Bragg's angle,D = Nanoparticle size in nanometer. A decrease in the average particle size with increasing Mn content is observed. The decrease in average particle size might be due to development of strain in the films because of Mn incorporation. The average particle size obtained for un-doped and different compositions of $Zn_{1-X}Mn_XO$ are 19, 18, 15 and 13 nm for x = 0, 3, 6, 9%, respectively.

$$D = K\lambda/\beta \cos \Theta \quad \text{……..(5)}$$

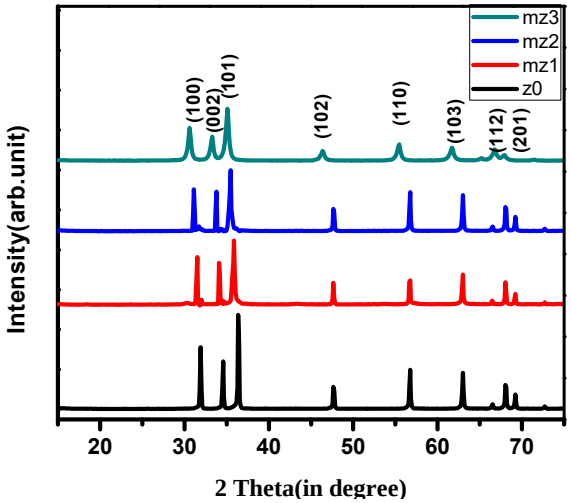

Fig 1: XRD pattern of Samples (a) ZO, (b) MZ1, (c) MZ2 and (d) MZ3

3.2 Surface Morphology

Surface morphological studies of un-doped and Manganese doped ZnO were carried out by scanning electron microscopy.Fig.2 (a-d) shows the Scanning electron micrographs of un-doped and Mn doped ZnO films at different magnifications. The SEM picture revealed the formation of uniform and dense interconnected web-like structure with porous morphology. Such dense films usually have superior mechanical, optical and electrical properties [17]

The interconnected webs with different pore diameter were observed in Fig 2. It may be due to the sequential growth of webs, one above another during growth process. Porosity of the synthesized material may be suitable for the gas sensing application. It causes to increases electron channels between adjacent pore surface and constructs good network. Such network helps to enhance the performance of gas sensitivity response specially response time and sensitivity. Porosity and homogeneity of the deposited film are desired for adsorption to certain gas. [18-19].

3.4 Energy dispersive X-Ray Analysis

EDAX spectra of un-doped sample shows a sharp peak of ZnO without any impurity and that of Mn doped ZnO data clearly show peaks corresponding to elements Zn, Mn and O. Table 1 provides the compositional percentage of chemically synthesized un-doped and Mn doped ZnO samples synthesized by Combustion methods. The EDX analysis indicates precise composition of the elements.

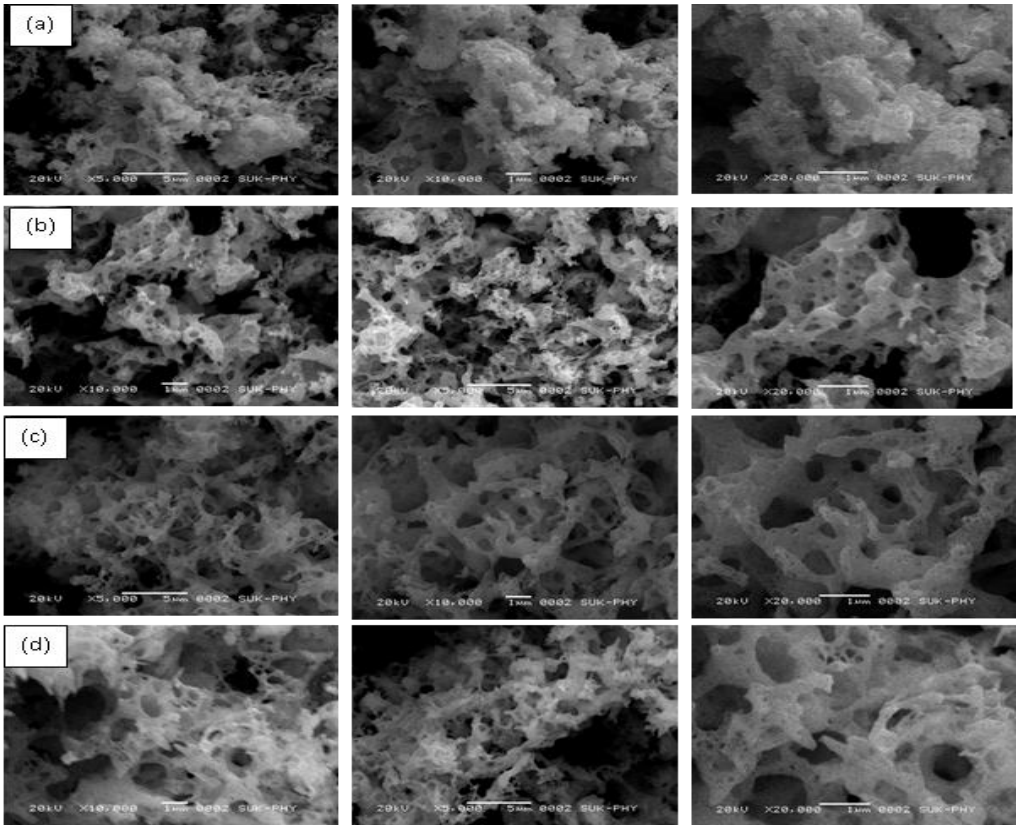

Fig 2: Scanning electron microscope images of Sample (a) Z0 (b) MZ1(c) MZ2 (d) MZ3

Samples →	Z0	MZ1	MZ2	MZ3
Elements ↓	At %	At %	At %	At%
O	61.55	65.25	65.84	69.81
Mn	00.00	01.49	02.31	03.01
Zn	38.45	33.27	31.85	27.29
Total	100	100	100	100

Table 2 : EDAX Data shows elemental composition of sample

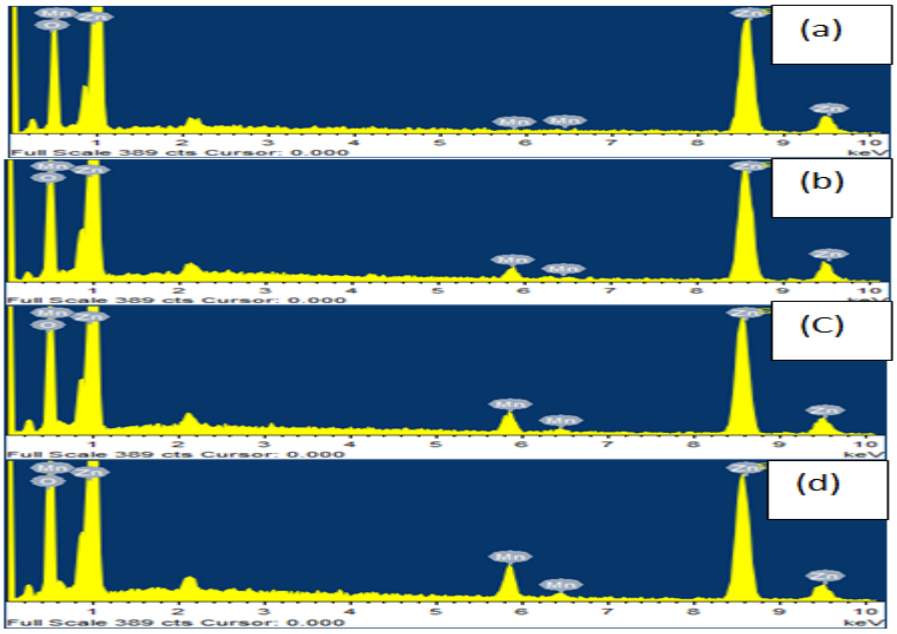

Fig 3 : EDAX of Sample (a) Z0 (b) MZ1(c) MZ2 (d) MZ3

3.5 UV- Visible

The plots of $(\alpha h\nu)^2$ versus hν of the un-doped and Mn-doped ZnO thin films are shown in Fig 4 The absorption spectra of un-doped and Mn-doped ZnO thin films were studied without taking into account of reflection and transmission losses.It is seen that with the increase of manganese doping level, the fundamental absorption edge decreases. The value of *Eg*for un-doped ZnO is 3.3 eV. It decreases to 2.45, 2.38 and 2.32 eV for 3%, 6% and 9% Mn doped ZnO respectively. This behavior of decrease in band gap was explained by using simple model [20]. According to these model periodic variations in potential within the grain occurs due to trapping of impurities introduced as a result of doping. Such periodic variation of potential, further leads to the band bending or band tailing effect [21-23]. Impurity band formation is an obvious consequence of increased doping concentration [24] and the trapping of the Mn atoms at the grain boundary leads to the introduction of the Mn defect states within the forbidden band. With increasing Mn doping, density of this Mn induced defect states increases, leading to the observed decrease of band gap.

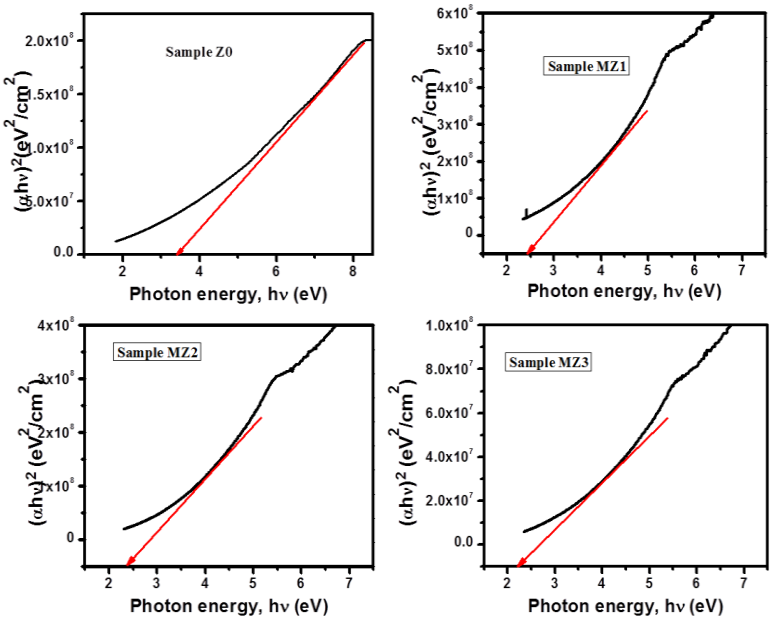

Fig 4: Optical study of samples Z0. MZ1, MZ2 and MZ3

IV. GAS SENSOR

4.1 Ammonia gas sensor mechanism

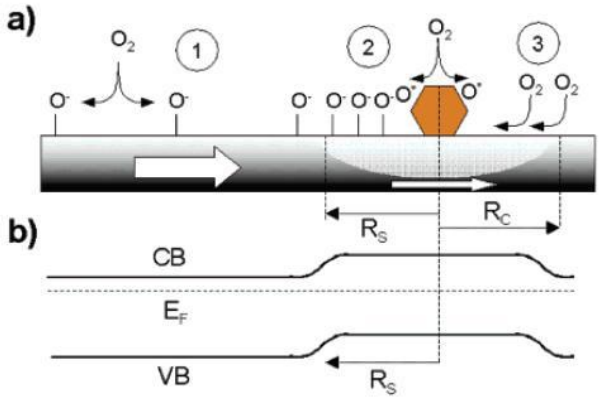

Fig 5: a) Schismatic diagram of processmechanism.when material exposed to O_2 and b) Band diagram

When the sensor is exposed in air and heated to 373-473K, the oxygen molecules in the atmosphere are adsorbed onto surfaces of the nanoporous web network, are transforming into oxygen ion molecules (Eq.(1). As temperature increases to 523–623 K, these oxygen molecules are dissociated into oxygen ions with a singly or doubly negative charge through depriving electrons from the ZnO conduction band (CB) "Equation. 6, 7 and 8", resulting in increase in resistance of the sensor. Once

the sensor is exposed in the reductive gas atmosphere such as ammonia, the oxygen ions on surfaces of nanoporous web network react with the ammonia molecules, retrieving the trapped electrons on the surfaces back to the CB of ZnO "Equation 9 and 10"such reaction leads to decrease in resistance (i.e., conductivity enhancement) for the ZnO gas sensors.

$$O_2(gas) + e^- \Leftrightarrow O_2^-(ads) \quad \ldots\ldots\ldots\ldots(6)$$

$$1/2O_2 + e^- \Leftrightarrow O^-_{ads} \quad \ldots\ldots\ldots\ldots(7)$$

$$1/2O_2 + 2e^- \Leftrightarrow O^{2-}_{ads} \quad \ldots\ldots\ldots\ldots(8)$$

$$4NH_{3ads} + 3O^-_{ads} \Rightarrow 2N_2 + 6H_2O + 3e^- \quad \ldots\ldots\ldots\ldots(9)$$

$$4NH_{3ads} + 3O^{2-}_{ads} \Rightarrow 2N_2 + 6H_2O + 6e^- \quad \ldots\ldots\ldots\ldots(10)$$

Gas-sensing mechanism of based on the two steps: (1) the diffusion of the analyte gas to the sensing surface and (2) decomposition of analyte gas on the surface. In the first step, it should be noted that the diffusing rate of gas is different. According to the Knudsen diffusion constant (D_K)"equation 11" [25]:

$$D_k = \frac{4r}{3}\sqrt{\frac{2RT}{\Pi M}} \quad \ldots\ldots\ldots\ldots(8)$$

Where, T represents operating temperature, M represents molecular weight and r represents pore radius. It is apparent from the above formula that, the pore radius highly impact on diffusing rate. Since sample MZ3 shows interconnected webs with larger pore size more gas molecules can quickly diffuse into deeper region. Furthermore, porous structure on the surface of element not only provides enough space to reduce space interruption induced by the gas adsorption, but also increases its inner surface, thus the gas can be adsorbed on the inner surface of the element through Van der Waals force. It could help to improve the gas adsorption ability and sensitivity. Also enhancement in sensitivity with doping might be due to fact that Mn is a far better oxygen dissociation catalyst than zinc oxide and catalytically activate the dissociation of molecular oxygen, whose atomic products then diffuse to the metal oxide support as shown in Fig.5 [26]. This process significantly increases both the quantity of oxygen that can repopulate vacancies on the ZnO surface and the rate at which this repopulation occurs, resulting in a greater degree of electron withdrawal from the ZnO. This mechanism is known as spillover mechanism [27]. An effective oxygen delivery system forms if the whole surface of metal oxide covered by this oxygen "collection zones" [28]

4.3 Effect of temperature

The sample MZ3 showed the well-developed interconnected web like structure with porous morphology and thus used to study the ammonia sensing properties at the beginning. Before exposing to ammonia gas, sample MZ3 was allowed to be stable for electrical resistance for half an hour and the stabilized resistance was taken as Ra. Fig 6 shows the response of sample MZ3 to 24 ppm of ammonia in air measured at different operating temperatures from 473K to 598 K.

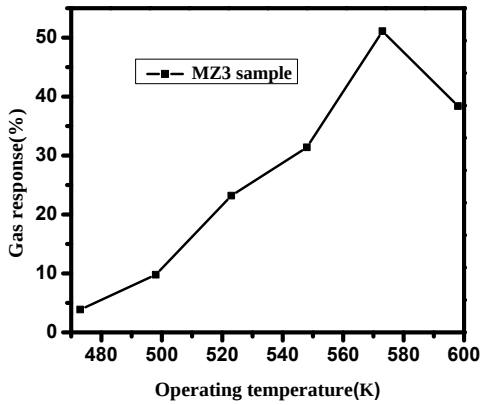

Fig 6: Dynamic sensing transient of sample MZ3 for ammonia gas at different operating temperature.

The temperature of the sensor surface is one of the major parameters. The temperature strongly affects on the physical properties of the semiconductor sensor material such as charge carrier concentration, Debye length, work function etc [28]. The optimum operating temperature for an effective sensor performance corresponds to that where the material is able to catalytically reduce or oxidize the target gas, simultaneously changing the electrical properties of the sensor material. Response of sensors depends on two factors, namely, the speed of chemical reaction on the surface of the grains, and the speed of the diffusion of gas molecules to that surface. These are activation processes, and the

activation energy of chemical reactions is higher. At low temperatures the sensor response is restricted by the speed of chemical reactions while at higher temperature it is restricted by the speed of the diffusion of gas molecules to that surface. At some intermediate temperature the speed values of two processes become equal, and at that point the sensor response reaches its maximum [29]. According to this mechanism for every gas there is a certain temperature at which the sensor response reaches its peak value. Above this maximum temperature, the gas response decreases due to desorption of the oxygen which are adsorbed on the surface of the sensor [30]. Another reason for the decrease in the gas response above the maximum temperature could be the increase in the carrier concentration due to intrinsic thermal excitation which decreases the Debye length [31].This length describes the size of the space-charge region next to the surface where the free carrier concentration may be affected by the surface species. In the present case it was observed that the sensor response increased from 3.84% to 51.11% as temperature increased from 473K to 573K for sample MZ3 and then decreases to 38.4% at 598K upon exposure of 24 ppm of ammonia gas concentration as shown in Fig.6. Therefore, the temperature 573K was taken as an optimum operating temperature for further studies. Once the operating temperature was fixed the sensor response was studied for different samples. From Fig.7 it is clear that un-doped sample of ZnO(Z0) showed response of 40.8% while 41.17% for sample MZ1 and 46.22% for sample MZ2 upon the exposure of 24 ppm of ammonia gas at 573K.

4.4 Effect of ammonia gas concentration

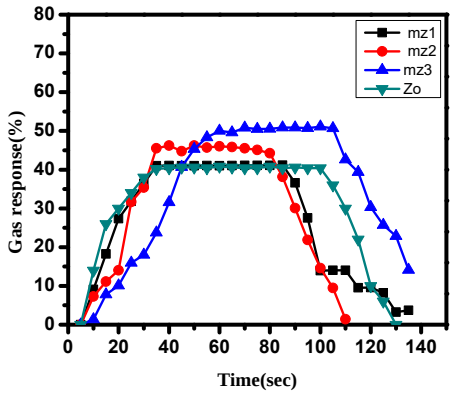

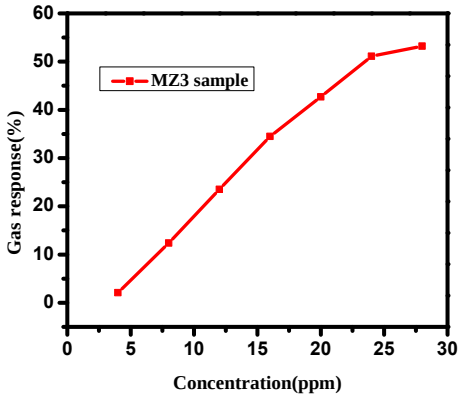

Figure 7: Dynamic sensing transient of ammonia gas for samples Z0, MZ1, MZ2 and MZ3 at operating temperature 573K.

Figure 8: Dynamic sensing transient of ammonia gas concentration for sample MZ3 at operating temperature 573K.

The dynamic variation of sensitivity of sample MZ3 with operating temperature of 573 K for different concentration of exposed ammonia is shown in Fig 8 Reveals that the response increased from 3.84% to 51.11% for the sample MZ3 as the ammonia concentration increased from 4 to 24 ppm. However, at higher concentrations the increase in gas response value was steady and saturated .The response of a sensor mostly depends on the removal of adsorbed oxygen molecules by reaction with a target gas and generation of electrons. For a small concentration of gas, exposed on a fixed surface area of a sample, there is a lower coverage of gas molecules on the surface and hence minor surface reaction takes place. An increase in gas concentration increases the surface reaction due to a larger surface coverage. A further increase in surface reaction will be gradual after saturation point of the coverage of molecules is reached.

4.4 Effect of doping on ammonia gas sensor

It has been observed that sensitivity increases with the Manganese doping concentration. The Sample Z0, MZ1, MZ2 and MZ3 showed ammonia gas sensitivity 40.8, 41.17, 46.22 and 51.11% Sample MZ3 showed maximum ammonia gas sensitivity of 51.11%. From observed SEM micrograph, it is evident that the pore diameter increases with Mn doping. The highest gas response may be due to high surface area availability and increase in pore size which provides the better electron channels between the web network as discussed in section 4.1.

V. CONCLUSION:

Un-doped and Mn doped ZnO nanoparticles were synthesized by Chemical Combustion method. The X-Ray diffraction study showed formation of hexagonal wurtzite crystal structure of Un-doped ZnO while Mn doped ZnO was polycrystalline.

Scanning electron microscopy revealed porous interconnected web like morphology with increase in pore size with increase in dopant concentration. Elemental composition was confirmed by EDAX. Optical data were shows decrease in band gap with increase in dopant percentage. Incorporation of Mn concentration in ZnO results enhanced gas response as Compared with un-doped ZnO, at relative lower concentration of ammonia gas. Also operating temperature is lowered. 9% Mn doped ZnO thin film showed the maximum gas response of 51.11% upon exposure to 24 ppm ammonia gas concentration at 573K temperature. The stability study indicates that Mn-doped ZnO is potential material for Ammonia sensing.

ACKNOWLEDGEMENT:

Author is gratefully thankful to University Grant Commission, New Delhi for sanctioning financial assistance under the scheme of minor research project.

REFERENCES

[1]. Khuspe G. D., Sakhare R. D., Navale S. T., Chougule M. A., Kolekar Y. D., and Mulik R. N., Nanostructured SnO 2 thin films for NO 2 gas sensing applicationsCeram. Int., 39(8) (2013) 8673–8679.

[2]. Rai P., Raj S., Ko K., Park K., and Yu Y., Sensor and Actuators B : Chem. Synthesis of flower-like ZnO microstructures for gas sensor applications178(2) (2013) 107–112.

[3]. Tao W. and Tsai C., "H_2S sensing properties of noble metal doped WO_3 thin film sensor fabricated by micromachining, Sensors Actuators B. Chem.81(55) (2002).

[4]. Bianchi S., Comini E., Ferroni M., Faglia G., Vomiero A., and Sberveglieri G., Indium oxide quasi-monodimensional low temperature gas sensor, Sensors Actuators B. Chem.118 (2006) 204–207.

[5]. Zhang Y., He X., Li J., Zhang H., and Gao X., Gas-sensing properties of hollow and hierarchical copper oxide microspheresSensors Actuators B. Chem. 128(1) (2007) 293-298.

[6]. Cristina M., Guidi V., Malag C., Vendemiati B., Zanni A., Martinelli G., Sacerdoti M., Licoccia S., Luisa M., Vona D., and Traversa E., Effects of Ta/Nb-doping on titania-based thin films for gas-sensingSensors Actuators B. Chem.108 (2005) 89–96.

[7]. Yu A., Qian J., Pan H., Cui Y., Xu M., Tu L., Chai Q., and Zhou X., Micro-Lotus Constructed by Fe-Doped ZnO Hierarchically Porous Nanosheets: Preparation, Characterization and Gas Sensing Property Sensors Actuators B. Chem.158(1) (2011) 9–16.

[8]. Yao M., Ding F., Cao Y., Hu P., Fan J., Lu C., Yuan, Shi C., and Chen Y., Sn doped ZnO layered porous nanocrystals with hierarchical structures and modified surfaces for gas sensors Sensors Actuators B. Chem.201 (2014) 255–265.

[9]. Shishiyanu S. T., Shishiyanu T. S., and Lupan O. I., Properties of SiO2 thin films prepared by anodic oxidation under UV illumination and rapid photothermal processing, Electrochim, Sensors Actuators B.Chem., 107(1) (2005) 379–386.

[10]. Baranowska-korczyc A., Fronc K., Pe J. B., Sobczak K., Klinger D., and Elbaum D., . Light- and environment- sensitive electrospun ZnO nanofibers Radiation Physics and Chemistry 93 (2013) 21–24.

[11]. Murugesan N. and Achuthanunni A., structural and optical properties of undoped and co-doped ZnO nanostructured thin films, Suranaree J. Sci. Technol. 18 (1) (2011) 81–88.

[12]. Poongodi G., Kumar R. M., and Jayavel R.,Enhanced antibacterial activity of transition metal doped ZnO nanorods on thin films, International J. of Chem tech research, 6(3) (2014) 2026–2028.

[13]. Hu P., Han N., Zhang D., Ho J. C., and Chen Y., Highly formaldehyde-sensitive, transition-metal doped ZnO nanorods prepared by plasma-enhanced chemical vapor depositionSensors Actuators B. Chem.,169 (2012) 74–80.

[14]. Sahay P.P., Nath R.K., Al-doped zinc oxide thin films for liquid petroleum gas (LPG) sensors,Sensors and Actuators B, 133 (1) (2008) 222-227.

[15]. Abdollahi Y., Abdullah A. H., Zainal Z., and Yusof N. A.,Synthesis and characterization of Manganese doped ZnO nanoparticlesinternational J. basic and applied Sci. Technol.11(4) (2011).

[16]. Duta A., TiO2 thin layers with controlled morphology for ETA (extremely thin absorber) solar cells, solar cells Thin Solid Films, 511 (2006) 195-198.

[17]. Zhu Y., Wang Y., Duan G., Zhang H., Li Y., Liu G., Xu L., and Cai W., Insitu growth ZnO nanosheet-built network film as high performance gas sensor, of porous Sensor Actuators B. Chem. 221 (2015) 350–356.

[18]. Gürbüz M., LPG sensing characteristics of electrospray deposited SnO_2 nanoparticles, Applied Surface Science, 318 (2014) 334–340

[19]. Suryanarayan C., Grant M. Norton, 'X-Ray Diffraction: A Practical Approach',(Plenum Press, New York.1998)
[20]. Singh P.,Kaushal A., Kaur D., Mn-doped ZnO nanocrystalline thin films prepared by ultrasonic spray pyrolysis", J Alloys and Compounds,471 (2009) 11.
[21]. Tauc J., Grigorvici R., Yanca Y., Optical Properties and Electronic Structure of Amorphous germanium Physica Status Solidi 15 (1966) 627.
[22]. Bandyopadhyay S., Paul G. K., Sen S. K., Study of optical properties of some sol–gel derived films of ZnO, Solar Energy Materials & Solar Cells, 71 (2002) 103.
[23]. Pancove J. 'Optical Processes in Semiconductors', (Prentice-Hall, Englewood Cliffs, NJ.1979)
[24]. Tian S., Ding X., Zeng D., Zhang S., Xie C., Sens. Pore-size-dependent sensing property of hierarchical SnO 2 mesoporous microfibers as formaldehyde sensorsActuators, B: Chem. 186 (2013) 640–647.
[25]. Kolmakov A., Klenov D. O., Lilach Y., Stemmer S., Enhanced gas sensing by individual SnO2 nanowires and nanobelts functionalized with Pd catalyst particles, Nano Lett.5 (2005) 667-673.
[26]. S. Khoobiar, Particle to particle migration of hydrogen atoms on platinum—alumina catalysts from particle to neighboring particles J. Phys. Chem., 68 (1964) 411.
[27]. Tsu K., Boudart M., Recombination of Atoms at the Surface of Thermocouple Probes.J. Chem.,39(1961)1239-1246.
[28]. Nenov T.G., Yordanov S.P., Ceramic Sensors, Technology and Applications (Technomic Pub., Lancaster**,** 1996).
[29]. Windichamann H., Mark P., A Model for the Operation of a Thin-Film SnOx Conductance-Modulation Carbon Monoxide Sensor J. Electrochem. Soc.4, (1979) 627–633.
[30]. Mizsei J., How can sensitive and selective semiconductor gas sensors be made?Sens. Actuat. B 23(1995) 173–176.
[31]. Hieu N. V., Quang V.V., Hoa N.D., Kim D., Preparing large-scale WO 3 nanowire-like structure for high sensitivity NH 3 gas sensor through a simple route, Curr. Appl. Phys., 11 (2011) 657–661.

International Journal of Engineering Research and Applications (IJERA) is **UGC approved** Journal with Sl. No. 4525, Journal no. 47088. Indexed in Cross Ref, Index Copernicus (ICV 80.82), NASA, Ads, Researcher Id Thomson Reuters, DOAJ.

K S Pakhare. "Highly porous web network of Mn doped ZnO for ammonia gas sensor." International Journal of Engineering Research and Applications (IJERA) , vol. 7, no. 9, 2017, pp. 06–14.